Available online at www.sciencedirect.com

## SciVerse ScienceDirect

journal homepage: www.elsevier.com/locate/jmbbm

**ELSEVIER**

Research paper

# Tunable nanomechanics of protein disulfide bonds in redox microenvironments

Sinan Keten[a,b], Chia-Ching Chou[a], Adri C.T. van Duin[c], Markus J. Buehler[a,d,*]

[a] Laboratory for Atomistic and Molecular Mechanics, Department of Civil and Environmental Engineering, Massachusetts Institute of Technology, 77 Massachusetts Ave., Room 1-235A&B, Cambridge, MA 02139, United States
[b] Department of Civil & Environmental Engineering and Mechanical Engineering, 2145 Sheridan Road, Northwestern University, Evanston, IL 60208-3109, United States
[c] Department of Mechanical and Nuclear Engineering, Pennsylvania State University, 136 Research Building East, University Park, PA 16802, United States
[d] Center for Materials Science and Engineering, Massachusetts Institute of Technology, 77 Massachusetts Ave., Cambridge, MA 02139, United States

## ABSTRACT

Disulfide bonds are important chemical cross-links that control the elasticity of fibrous protein materials such as hair, feather, wool and gluten in breadmaking dough. Here we present a novel computational approach using the first-principles-based ReaxFF reactive force field and demonstrate that this approach can be used to show that the fracture strength of disulfide bonds is decreased under the presence of reducing agents, due to a loss of cross-link stability controlled by the chemical microenvironment. Simulations in explicit solvents and dithiothreitol (DTT) indicate an intermediate step involving weakened elongated bonds, illustrating the tunability of the elasticity, rupture mechanism and strength of proteins. We provide a mechanistic insight into the fracture mechanism of protein disulfide bonds and illustrate the importance of the redox microenvironment, where factors such as accessibility, mechanical strain and local redox potential govern the dominating rupture mechanism and location. The method used here provides a general computational protocol for studying mechanochemical fracture of large-scale protein materials concurrently with experimental efforts.

© 2011 Elsevier Ltd. All rights reserved.

## 1. Introduction

Cysteine (abbreviation CYS) exists in about 20% of all proteins, and plays a fundamental role in structure, flexibility and mechanical properties of biological materials (Brändén and Tooze, 1999; Voet and Voet, 2004; Cheek et al., 2006; Fratzl and Weinkamer, 2007; Buehler and Yung, 2009; Garcia-Manyes et al., 2009). This is because in oxidising environments, sulfur side-chain atoms in cysteine can form intramolecular disulfide (S–S) bonds, creating a reversible cross-link that

can be broken under the presence of a reducing agent. Thereby, disulfide bonds provide tunable stability to folded structures of proteins, enabling specific mechanical functions such as molecular sensing, switching and signalling in biology (Aslund and Beckwith, 1999; Mayans et al., 2001; Hogg, 2003). From a physical chemistry perspective, intermolecular contacts formed via sulfur atoms control the elasticity protein and polymeric materials such as breadmaking dough (Shewry and Tatham, 1997), vulcanised rubber (Flory, 1953), and define the unique hierarchical features of hair, feather, beak and wool (Parbhu et al., 1999; Wang et al., 2000; Mayans et al., 2001; Mucke et al., 2004). Oxidative stress conditions related to diseases (e.g. diabetes, cardiovascular disease) and aging (Cumming et al., 2004) also involve disulfide bonds, where reactive oxygen species are believed to speed up ageing as they change the chemical structure of proteins via the formation and stabilisation of cross-links. Overall, disulfide bond chemistry and mechanics are fundamental to our understanding of molecular, cellular and tissue level properties of biological materials in both physiological and disease conditions.

Facilitated by recent advancements in experimental techniques, pioneering studies of thiol–disulfide exchange reactions under external force application and the presence of dithiothreitol (DTT) have demonstrated a rate-dependent bond rupture mechanism that can be described by the Bell model (Bell, 1978; Wiita et al., 2006). Other reducing agents, such as thioredoxin enzymes found in prokaryotic and eukaryotic cells, show a variety of complex chemical reaction pathways that boost the rate of reduction in biological systems (Wiita et al., 2007; Perez-Jimenez et al., 2009). A major limitation to computational studies of disulfide bonds is that the rupture of covalent bonds cannot be simulated via the classical force fields such as DREIDING, CHARMM or AMBER (MacKerell et al., 1998; Ponder et al., 2003), since covalent bonds are typically treated as unbreakable harmonic springs. Previous computational studies on disulfide bond properties have been limited to small systems with often only tens to hundreds of atoms, where Density Functional Theory (DFT) or Car–Parrinello Molecular Dynamics (CPMD) and QM/MM methods have been employed to investigate potential reaction pathways (Li and Grater, 2010; Fernandes and Ramos, 2004; Hofbauer and Frank, 2010). Studying disulfide bond dynamics beyond the single molecule level remains a computational challenge, due to the prohibitive cost of quantum calculations. As a result, efficient interatomic MD force fields are in demand to extend the length and time-scale of simulations involving chemical reactions.

Here we report progress in addressing this challenge for proteins using molecular dynamics simulations with the ReaxFF reactive force field (van Duin et al., 2001). ReaxFF is derived from first-principles calculations and is capable of modelling chemical reactions (including transition states during reactions, changes in bond order, charge equilibration) while retaining computational efficiency, which has been previously demonstrated for a variety of reactive systems including oxidisation of hydrocarbons, silicon fracture and catalysis of carbon nanotube formation (Nielson et al., 2005; Buehler et al., 2006; Chenoweth et al., 2008). We consider a simple model system consisting of two cysteine amino
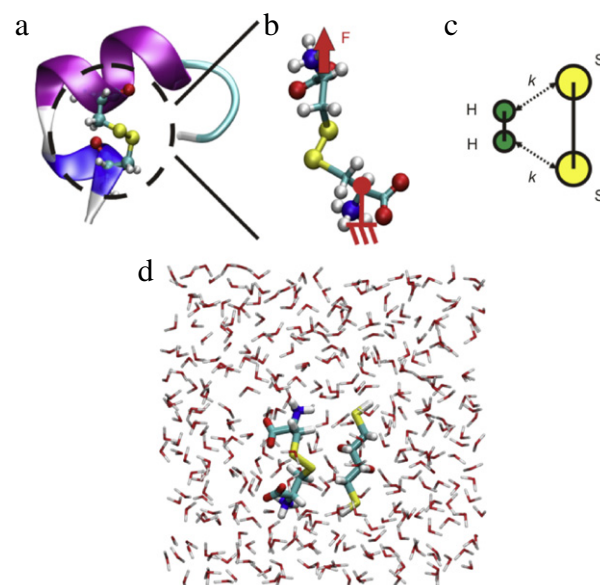


Fig. 1 – Schematic views illustrating the simulation setup. The disulfide bond model is taken from a small protein (Protein Data Bank identification code 1AKG) shown in panel A. Steered Molecular Dynamics simulations are carried out, where one of the amino acids is fixed and the other is pulled at the alpha-carbon atom as depicted in panel B. Panel C shows the method for inducing reactions. To induce a reducing potential, hydrogen atoms (in the schematic shown as a hydrogen molecule) are tethered towards the S–S bond with a harmonic bias potential, thereby sampling the reaction at a shorter time-scale accessible to Molecular Dynamics. Panel D shows the overall system solvated in an explicit water box (approximately 1000 atoms) with periodic boundary conditions.

acids covalently linked by a single disulfide bond to gain a fundamental insight into the nanomechanics of disulfide bonds in proteins under varied chemical and physical conditions. Fig. 1(A) and (B) show the general molecular setup and simulation protocol. As depicted in Fig. 1(C), reactions are explored by using a variable biasing potential that tethers the hydrogen atoms to the sulfur atoms to enhance the sampling of reactions (Laioa and Parrinello, 2002; Bonomi et al., 2009; Bonomi and Parrinello, 2010). All simulations are carried out in a periodic box of water with explicit solvent, as shown in Fig. 1(D) in a system containing about 1000 fully reactive protein and water solvent atoms, to capture solvent effects (hydrophobicity, viscosity, screening, possible reactions etc.) accurately. Details of the computational approach are provided in the materials and methods section.

## 2. Materials and methods

### 2.1. Molecular simulation approach

Molecular Dynamics simulations are carried out using the LAMMPS software (Plimpton, 1995) with ReaxFF (van Duin

et al., 2001) and Steered Molecular Dynamics (Isralewitz et al., 2001) packages. Simulations are carried out for a simple protein system consisting of two cysteine amino acids linked via a disulfide bond. The initial atomic coordinates of the model are obtained from the alpha-connotoxin protein (Protein Data Bank identification code 1AKG) in the Protein Data Bank (Bernstein et al., 1977). The system is solvated within a box of explicit reactive water using Visual Molecular Dynamics (Humphrey et al., 1996). Each simulation is carried out in explicit solvent within a periodic simulation box (approximately containing 1000 atoms), using the recently developed ReaxFF parameter set for proteins (Rahaman et al., 2011). A Steered Molecular Dynamics approach is used to provide external mechanical perturbation to the system, to induce the breaking of the peptide chain. The Steered Molecular Dynamics spring constant is set as $10\,\text{kcal/mol/Å}^2$ and the pulling velocity is 0.05 Å/ps. All visualisations are done using the Visual Molecular Dynamics software (Humphrey et al., 1996). For the simulations with bias potentials, reactions are driven varying the equilibrium length (sliding restraints) or force constant of the springs systematically over several simulations.

## 2.2. Research design

We study several cases designed to assess the rupture mechanisms of disulfide bonds under combined mechanical forces and reducing agents and using different harmonic bias potentials to sample varied time-scales. The bias potentials used here are implemented as harmonic functions defined as $E_{bias} = \frac{1}{2}k(R - R_0)^2$ where $R$ is the distance between the pair of atoms, and $R_0$ denotes the target distance between the pair of atoms. The parameter is a constant that defines the strength of the bias potential (referred to as the "bias potential constant"). The goal of these simulations is to quantify the mechanical rupture strength and rupture point of the cysteine molecule in conditions that mimic a variety of redox chemical environments. The first case involves stretching simulations of the cysteine molecule in the close presence of molecular hydrogen (reducing agent) and molecular oxygen (oxidising agent). The $O_2$ or $H_2$ molecule is biased to the sulfur atoms in the protein with harmonic bias potentials that have gradually increasing bias potential constants. The purpose of this investigation is to probe the reduction of the disulfide bond with hydrogen and oxygen molecules, and show that in the false test of oxygen, the reduction of the S–S- bond cannot occur regardless of the biasing function.

The second set of simulations involves the behaviour of cysteine in the presence of deprotonated dithiothreitol (DTT). In umbrella sampling simulations, we vary the equilibrium length of the bias potential ($k = 5, 10\,\text{kcal/mol/Å}^2$) range of values chosen between 1 and 10 Å to control the position of the DTT molecule with respect to the protein. The goal of this setup is to evaluate the role of the access of the DTT molecule to the disulfide bond on the fracture mechanics of the protein. This is very relevant for physiological proteins that have buried disulfide bonds, which are non-reducible unless denatured.

Our simulations employ an NVT ensemble with a temperature set at 300 K, with an integration time

step of 0.25 fs. We run 27 simulations with typical simulation time-scales from hundreds of picoseconds to a few nanoseconds, depending on the bond rupture time-scale under mechanical strain and biasing potentials. Post-processing of umbrella sampling simulations (results shown in Fig. 4(B)) is carried out using the weighted-histogram analysis method (WHAM, http://membrane.urmc.rochester.edu/Software/WHAM/WHAM.html, Grossfield, 2008).

## 2.3. Mechanical strength analysis

We study the maximum force of disulfide bond breaking under mechanical force applied with hydrogen and oxygen molecules, respectively. To sample the reaction at longer time-scales, two bias potentials are applied between pairs of each of the sulfur atoms (of the disulfide bond) and corresponding hydrogen/oxygen atoms in the system. To achieve this bias potentials are added between S–O and S–H for the two cases investigated. The bias potential is implemented as described above. In order to assess the mechanical force needed to break the disulfide bond and to examine associated cleavage mechanisms under $H_2$ or $O_2$ presence, we vary the effect of the bias potential and compute the maximum force of the bond breaking with $H_2$ and $O_2$. We systematically vary the bias potential constant $k$ from 1 to $50\,\text{kcal/mol/Å}^2$ while keeping all other parameters constant. The alpha-carbon atoms at the cysteine dimer are pulled on by using Steered Molecular Dynamics (Isralewitz et al., 2001) with a spring constant of $10\,\text{kcal/mol/Å}^2$ and the pulling force $F$ is recorded versus the position. All simulations are carried out at a pulling velocity of 0.05 Å/ps.

## 2.4. Metadynamics analysis

We use the metadynamics method to investigate the energy barrier of our system along collective variables (CVs). The metadynamics algorithm is implemented in a portable plug-in, the PLUMED package (Bonomi et al., 2009), which can be included in the LAMMPS software. During the simulation, an external bias potential, $V(s, t)$, is developed as a sum of Gaussian functions centred on visited configurations $s^{(0)}$ in the collective variables space, $s$, where

$$V(s, t) = \sum_{\substack{t' = \tau, 2\tau, 3\tau, \ldots \\ t' < t}} W \exp\left(-\sum_{i=1}^{d} \frac{\left(s_i - s_i^{(0)}(t')\right)^2}{2\sigma_i^2}\right) \qquad (1)$$

in which $s_i$ is the $i$th CV, $\sigma_i$ is the Gaussian width corresponding to the $i$-th CV, $W$ is the Gaussian height, $d$ is the number of collective variables and $\tau$ is the deposition frequency of the Gaussian. Eventually, the free energy of the system is obtained by

$$V(s, t) = -F(s, t). \qquad (2)$$

To investigate the effect of the bias potential on the energy barrier of cysteine with different agents, we perform metadynamics calculations using the S–S distance of the two cysteine residues as the only CV with different spring constants of bias potential for oxygen and hydrogen molecules. All calculations are performed with a Gaussian height, $W = 0.1\,\text{kcal/mol}$, width of 0.35 Å and a simulation time of 375 ps.

### 2.5. *Force field development and validation*

Unlike most classical Molecular Dynamics formulations that employ harmonic bond potentials and static charges (such as DREIDING or CHARMM), ReaxFF takes into account changes in charge distribution as well as changes in bond order (for example, $C \equiv C$ to $C=C$ to $C–C$) and is thus a fully reactive implementation capable to describe the covalent chemistry needed for complex reactions such as the breaking of disulfide bonds in proteins. ReaxFF simulations consider all atoms as reactive at all time steps and we do not use mixed reactive/non-reactive formulations in our simulations (no switching functions for bond reactivity or regional definitions are employed). We use the same force field constants in all simulations, that is, force field parameters are not varied to induce bond breaking. The ReaxFF parameters used in these simulations are solely based on quantum mechanical input, and were trained earlier against a DFT-based dataset, obtained at the B3LYP/6-311G** level of theory (Krishnan et al., 1980; Becke, 1993).

For all bonds, valence angles and dihedral angle types relevant to protein systems, a set of DFT-data was obtained tracking the system energy as a function of the internal coordinate. For example, for the S–H bond we used an $H_2$ S-molecule where the H–S bond was stretched from 0.7 to 4.0 Å, while the rest of the molecule was minimised. In addition, we used DFT data describing the concerted proton transfer barriers in $[H_2O]_n$ oligomers ($n = 2–6$), proton transfer in $H_2O–H_3O^+$ complexes and binding energies for hydrogen-bonded complexes to further constrain the ReaxFF parameters. The development of this parameter set and the numerical parameters are described in more detail elsewhere (Rahaman et al., 2011). To test the validity of these ReaxFF parameters for disulfide cleavage reactions we perform a ReaxFF reaction scan for thiol/disulfide exchange reaction, catalysed by a $H_2O/NH_3$ complex (Fig. 2). We find a barrier for this reaction of 28 kcal/mol, which is in excellent agreement with the thiol/disulfide exchange DFT results reported by Fernandes and Ramos (2004). This calculation is repeated for the cystine–DTT reaction. We also performed simulations with capped cysteine terminals and obtained similar results to the ones reported here.

## 3. Results and discussion

We start with an analysis of molecular hydrogen and oxygen attacking the disulfide bond, to assess bond rupture strengths and locations in representative oxidising and reducing conditions. Fig. 3(A) depicts snapshots from the simulation of disulfide rupture under reducing conditions, illustrating the reduction mechanism of the disulfide bond in the presence of a hydrogen molecule. Mechanical stretching of the system leads to exposure and straining of the disulfide bond. Before the reaction occurs, the bond is slightly elongated due to the presence of hydrogen atoms, which weakens the S–S bond. This is followed by the reduction of the sulfur atoms and fracture of the protein at the S–S bond. Next we carry out an identical simulation setup, but this time we replace the hydrogen molecule with an oxygen molecule (Fig. 3(B)). In
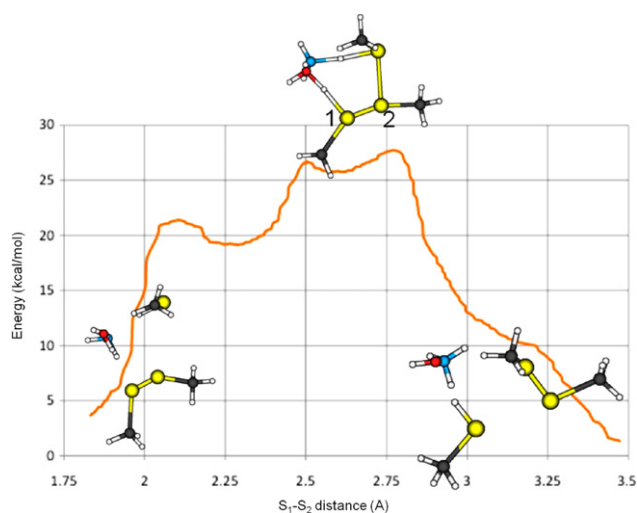


**Fig. 2 – ReaxFF reaction path for a thiol/disulfide exchange reaction, catalysed by a hydrogen bonded $H_2O/NH_3$ complex. These results are obtained from a low-temperature Molecular Dynamics simulation ($T = 10$ K) using sliding bond-restraint bias potentials to drive the formation and dissociation of the bonds involved in the reaction path. This simulation is used to identify the potential energy landscape during the chemical reaction and to validate ReaxFF parameters which are based on DFT calculations for thiol/disulfide exchange reactions that are carried out at similar low temperature conditions. (The other ReaxFF simulations reported in this paper are done at 300 K.)**

this case, regardless of the proximity of the oxygen molecule to the S–S bond, rupture of the S–S bond does not occur, which is in direct contrast to the hydrogen molecule case presented previously (Fig. 3(A)). Indeed, this is expected from basic redox chemistry, since further oxidation of a disulfide bond via a reaction with oxygen is unlikely. An interesting observation is that in this scenario, the large mechanical forces induce breaking of the adjacent C–S bond, rather than the S–S bond, a result that we also observe consistently in pure mechanical stretching of the dimer in solvent. These findings agree with previous theoretical predictions based on quantum mechanical methods that have also suggested the comparable bond energy and rupture likelihood of the C–S bond under external forces (Hofbauer and Frank, 2010). Therefore, the variation of the fracture location is a result arising most likely from enthalpic considerations in non-reducing conditions.

To directly demonstrate the effect of reducing agent on mechanics, we designed a setup in which we pull the ends of the protein using Steered Molecular Dynamics at a constant rate, while adding a bias potential between the sulfur atoms of the disulfide bond and an attacking molecule (here, $H_2$ and $O_2$ molecules are used as simplified models for reducing and oxidising agents). The bias potential has a varied strength to model sampling at different effective time-scales, arising from modified effective collision frequency in analogy to the Arrhenius description. Fig. 4(A) shows the breaking force as a function of the bias potential constant and reflecting
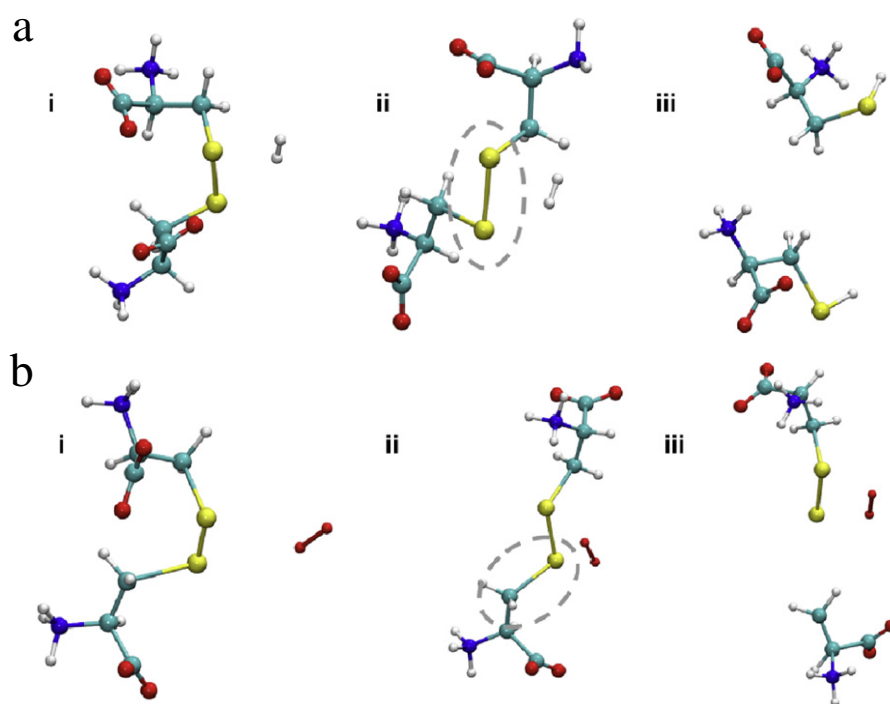
**Fig. 3 – Reaction mechanisms with molecular hydrogen and oxygen. Rupture mechanism of the disulfide bond depends on the local redox microenvironment, mimicked here by the presence of a tethered molecular oxygen (oxidising agent) or molecular hydrogen (reducing agent) in the vicinity of the disulfide bond. Dissociation of the hydrogen atom occurs simultaneously with the rupture of the S–S bond as shown in panel A (i–iii), forming stable reduced monomers of cysteine. We carry out an identical simulation, this time replacing hydrogen with an oxygen molecule. Since oxygen is an oxidising agent, a reaction with the disulfide bond does not take place. Instead, the adjacent C–S bond ruptures at very high mechanical forces as shown in panel B (i–iii). For clarity, surrounding water atoms are not shown.**

varied time-scales of observation. In the system with $O_2$, the C–S bond always breaks first and the strength does not seem to be influenced by the chemical environment significantly, since the cleavage of the S–S bond cannot be activated. On the other hand, the mechanism and force level of bond failure is quite strongly affected in the system with $H_2$ as a model reducing agent. As the bias potential constant increases – representing the behavior at longer time-scales – the force level of bond failure drops significantly, and the S–S bond always breaks first instead of the C–S bond. Fig. 4(B) shows representative force–displacement curves comparing the influence of $H_2$ and $O_2$. Because the accessible time-scales in molecular dynamics simulations is limited to nanoseconds and we successfully observe the thiol/disulfide exchange reaction in our simulations, the reaction would likely occur violently in the real time-scales once the molecules are in close proximity to each other. However, the difference of the bond breaking time-scale is hardly observed in experimental studies because the cleavage of a single bond usually happens in a very short time, whereas the diffusion of the molecules occurs at much longer time scales. Hence, the molecular dynamics simulations provide us with an opportunity to explore the detailed configuration changes during the reaction. It is worth noting here that the temperature plays a key role during a chemical reaction. From Bell's theory (Bell, 1978), for example, raising the temperature will likely decrease the bond lifetime, as it increases the

vibrational excitation of the S–S bond and also favors the high-entropy broken-bond state. Therefore, in a system at a higher temperature, the breaking force for a disulfide bond would be smaller than the breaking force shown in Fig. 4.

The curves show a much lower peak force and earlier rupture due to the presence of $H_2$. To solidify our findings, we also perform metadynamics simulations to obtain the free energy landscape of each system with a bias potential between the sulfur atoms of the disulfide bond and an attacking molecule ($H_2$ and $O_2$ molecules). The results of the resulting energy barriers are listed in Table 1. In the systems with $O_2$, the disulfide bond remains stable with an increasing bias potential. On the other hand, as the bias potential constant increases in the system with $H_2$, the energy barrier drops drastically, in agreement with the results shown in Fig. 4 where a smaller force is shown to be adequate to overcome the effective energy barrier. These results have two important implications. First, they directly show that the presence of a reducing agent leads to a significant reduction in the force required to break the disulfide bond. Second, these results suggest that the behavior of disulfide bonds is ultimately time-scale-dependent, where the weakening effect of the reducing environment is only seen at longer effective sampling times, as shown here qualitatively through the use of bias potentials. This indicates that the mechanics of disulfide cross-links are rate-dependent; similar to the observations made on weaker protein interactions such as
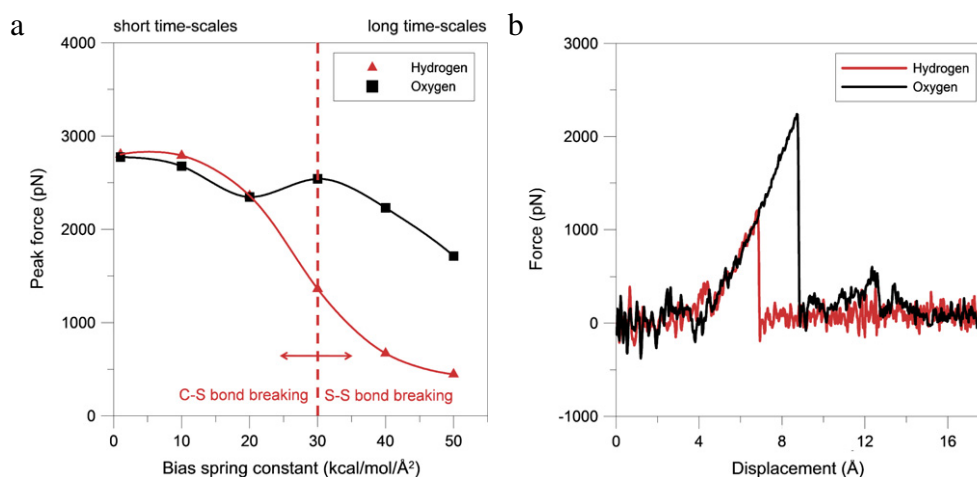
Fig. 4 – **Changes of nanomechanical strength properties of disulfide bond under presence of a reducing and oxidising agent. Panel A: breaking force as a function of the bias potential spring constant. This plot shows the bond breaking force is strongly dependent on the presence of a reducing or oxidising environment. In the system with $O_2$, an oxidising environment causes a small reduction in strength, but the C–S bond always breaks first. In stark contrast, the system with $H_2$ shows that the mechanism and force required to induce bond breaking is strongly affected in a reducing environment. As the bias potential constant increases (representing the behaviour at longer time-scales) the peak forces drop to significantly smaller levels than in the oxidising environment and the S–S bond breaks first, rather than C–S bond. The fitting function of the trend lines is a cubic spline function. Panel B: force–displacement curve showing a comparison of systems with $H_2$ and $O_2$ at a fixed bias potential constant of 30 kcal/mol/$Å^2$. The result shows a much lower peak force due to the presence of $H_2$, very different from the $O_2$ case, with a reduction by 45%). (Each data point is an average of every ten points of data.)**

Table 1 – **The energy barrier of disulfide bond rupture under the hydrogen and oxygen molecules. This table shows the energy barrier is strongly dependant on the presence of a reducing or oxidising environment. In the system with $O_2$, the energy barriers fluctuate in the range of 39–68 kcal/mol, but the larger spring constant does not cause a smaller energy barrier. Conversely, the system with $H_2$ shows that the reducing environment weakens the stability of the disulfide bond. The energy barriers drop dramatically while the bias potential constant increases.**

| Case considered | Bias potential spring constant (kcal/mol/$Å^2$) | | | | |
|---|---|---|---|---|---|
| | 1 | 10 | 20 | 30 | 40 |
| Protein with molecular oxygen, $O_2$ | 43.0 | 39.0 | 68.0 | 46.1 | 51.8 |
| Protein with molecular hydrogen, $H_2$ | 48.4 | 55.0 | 30.6 | 26.2 | [a] |

[a] As the spring constant is equal to $\approx 40$ kcal/mol/$Å^2$, the energy minimum is located at a S–S distance of 15 Å, and the S–S bond breaks spontaneously.

hydrogen bonds (Brockwell et al., 2003; Ackbarow et al., 2007; Dietz and Rief, 2008; Keten and Buehler, 2008).

While $H_2$ and $O_2$ are simplified choices for modeling reductive and oxidative microenvironments, a physiologically more relevant reaction is the nucleophilic attack by dithiothreitol (DTT) on a protein disulfide bond, which we investigate in this paper. DTT is much more reactive with proteins in its deprotonated form; therefore, we investigate the initiation of the reaction by introducing a deprotonated DTT in the vicinity of the disulfide bond. The strain on the dimer and the proximity of the DTT molecule can be modulated by systematically changing the bias potential equilibrium distance of the nucleophilic sulfur ($S_{nuc}$) as well as the two alpha-carbon atoms of the cysteine dimer. Fig. 5(A) illustrates a time sequence of events for the reaction that occurs between the deprotonated form of DTT and cysteine. This model setup is designed to quantify the accessibility required by the DTT molecule to carry out a nucleophilic

attack leading to an $S_N2$ substitution on a disulfide bond under mechanical strain. Fig. 5(B) shows the distribution of inter alpha-carbon distance and $S_{nuc}$–S distance on a free energy color map obtained from weighted-histogram analysis on the bias potential simulations (e.g. umbrella sampling, described in the materials and methods section). Based on these simulations, it is evident that partial bonding and elongation of the disulfide becomes favourable as slight molecular strain is introduced by displacing the alpha-carbon atoms further than their original length. In the case of DTT in close proximity of the molecule, the $S_{CYS}$–$S_{CYS}$ bond softens and shifts to an intermediate state, where $S_{nuc}$–S–S form elongated bonds. This state can be followed by the fracture of the dimer via the rupture of the original S–S bond if further strain is applied, or enough time passes for the complete nucleophilic substitution to take place. Regardless of the mechanical strain on the dimer, no bonding will occur if DTT cannot access cysteine (e.g. if the $S_{nuc}$–S distance
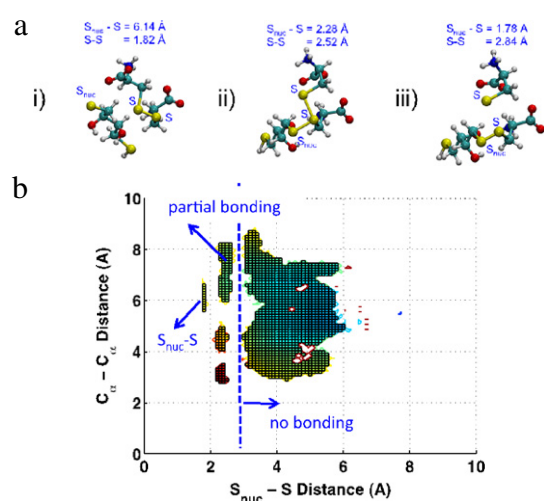
**Fig. 5 – Analysis of the reaction of DTT with cystine. We investigate the protein disulfide bond and DTT reaction mechanisms by varying bias potentials systematically to sample different extension states and accessibility conditions. Snapshots shown in panel A depict (i) the initial state, (ii) bond lengths at the intermediate state, and (iii) the final configurations of a reaction. Panel B summarises the distribution of inter alpha-carbon distance and nucleophilic sulfur ($S_{nuc}$) proximity observed in a collection of simulations with variable bias potentials. When the DTT molecule is further than 3 Å, reduction cannot occur and the molecular system samples a range of configurations. If the DTT molecule is in the proximity of the disulfide, then an intermediate partial bonding state is observed, which can lead to full bonding characterised by a further decrease in the $S_{nuc}$–S distance. The close presence of DTT weakens the S–S bond and causes elongation to approximately 2.5 Å thereby leading to an overall softening at this point. Further stretching leads to fracture via cleavage of the S–S bond.**

remains greater than approximately 3 Å), a scenario that is relevant for buried disulfides in proteins. The observation of the partially bonded elongated state provides direct evidence for the strong coupling between the chemical environment and mechanics of a disulfide bond, where elongation of the bond by a fraction of an ångström would not be observed by application of force only, considering the high stiffness of covalent bonds. The computed energy barrier for this case is approximately 32 kcal/mol, much lower than the dissociation energy that would be observed without nucleophilic attack. We note that this value will be even lower if mechanical strain is applied directly to the disulfide bond and the nanosecond time-scale of the simulations is extended.

## 4. Conclusions

By using the first-principles-based ReaxFF reactive force field applied to studying tunable mechanochemistry of disulfide bonds in proteins, we showed that the stability of the disulfide bond is strongly influenced by the redox potential of the chemical microenvironment, where variations in the

concentration of reducing agents can trigger various fracture mechanisms in the protein. A direct simulation of the fracture strength showed that the presence of a reducing agent drastically changes the strength of a protein disulfide bond, and controls the rupture location of a bond (Fig. 4). The results of metadynamics simulations confirm our Steered Molecular Dynamics results and show that the reducing agent decreases the energy barrier of disulfide bond rupture.

For S–S bond rupture, the intermediate state for disulfide bond rupture involves elongation and partial bonding at an intermediate elongation state of approximately 2.5 Å depending on the reduction mechanism and geometry. Similarly, experimental studies have also indicated a transition to elongated disulfide bonds upon introduction of a reducing agent to the system (Wiita et al., 2006). A key mechanistic insight gained from our study is that the presence of a reducing agent elongates and softens the S–S bond with respect to the competing candidate for rupture, the C–S bond, facilitating concentration of mechanical force on the weakened bond. An important result is that a strong coupling exists between the actual mechanical strain distribution in proteins and the existing local chemical cues in their environment. As demonstrated here, the exact fracture mechanism of a protein as well as measured fracture forces will typically depend on (i) accessibility of the cross-link, (ii) strength of reducing agents, and (iii) loading rate, as well as other factors. In scenarios reminiscent of shock loading of proteins over short time scales, the likelihood of the C–S bond to rupture may increase as the reducing agents have less time to interact with the protein.

Overall, the first-principles-based ReaxFF reactive force field, combined with mechanical perturbation and long-time-scale structure and free energy sampling protocols (Bonomi et al., 2009; Bonomi and Parrinello, 2010) provides a computational approach for studying the link between chemistry and mechanics of protein materials in various physical and chemical environmental conditions. It should be noted here that the current formulation of the force field is a generic version for protein applications, and therefore may not capture all aspects of specific chemical reactions accurately. Future iterations will focus on fine-tuning of the force-field parameters to accurately describe a range of chemical reactions relevant to protein materials, and extending reactive capabilities to greater length and time-scales. Future computational studies of the structural dynamics of disulfide bonds subject to chemical cues will hopefully provide insight into the tunable mechanics of protein cross-links, a biological mechanism that could potentially be exploited in bioinspired polymers or targeted drug delivery systems (Bernkop-Schnürch et al., 1999; Leitner et al., 2003; Napoli et al., 2004; Albrecht and Bernkop-Schnurch, 2007; Cerritelli et al., 2007; Lv et al., 2010).

## Acknowledgements

REFERENCES

Ackbarow, T., Chen, X., et al., 2007. Hierarchies, multiple energy barriers, and robustness govern the fracture mechanics of {alpha}-helical and beta-sheet protein domains. Proceedings of the National Academy of Sciences 104 (42), 16410–16415.

Albrecht, K., Bernkop-Schnurch, A., 2007. Thiomers: forms, functions and applications to nanomedicine. Nanomedicine 2 (1), 41–50.

Aslund, F., Beckwith, J., 1999. Bridge over troubled waters: sensing stress by disulfide bond formation. Cell 96 (6), 751–753.

Becke, A.D., 1993. Density-functional thermochemistry. III. The role of exact exchange. Journal of Chemical and Physics 98, 5648.

Bell, G.I., 1978. Models for specific adhesion of cells to cells. Science 200 (4342), 618–627.

Bernkop-Schnürch, A., Schwarz, V., et al., 1999. Polymers with thiol groups: a new generation of mucoadhesive polymers? Pharmaceutical Research 16 (6), 876–881.

Bernstein, F.C., Koetzle, T.F., et al., 1977. Protein data bank—computer-based archival file for macromolecular structures. Journal of Molecular Biology 112 (3), 535–542.

Bonomi, M., Branduardi, D., et al., 2009. PLUMED: a portable plugin for free-energy calculations with molecular dynamics. Computer Physics Communications 180 (10), 1961–1972.

Bonomi, M., Parrinello, M., 2010. Enhanced sampling in the well-tempered ensemble. Physical Review Letters 104 (19), 190601.

Brändén, C.-I., Tooze, J., 1999. Introduction to Protein Structure. Garland Pub., New York

Brockwell, D.J., Paci, E., et al., 2003. Pulling geometry defines the mechanical resistance of a beta-sheet protein. Nature Structural Biology 10 (9), 731–737.

Buehler, M.J., van Duin, A.C.T., et al., 2006. Multiparadigm modeling of dynamical crack propagation in silicon using a reactive force field. Physical Review Letters 96 (9), 095505-4.

Buehler, M.J., Yung, Y.C., 2009. Deformation and failure of protein materials in physiologically extreme conditions and disease. Nature Materials 8 (3), 175–188.

Cerritelli, S., Velluto, D., et al., 2007. PEG-SS-PPS: reduction-sensitive disulfide block copolymer vesicles for intracellular drug delivery. Biomacromolecules 8 (6), 1966–1972.

Cheek, S., Krishna, S.S., et al., 2006. Structural classification of small, disulfide-rich protein domains. Journal of Molecular Biology 359 (1), 215–237.

Chenoweth, K., van Duin, A.C.T., et al., 2008. ReaxFF reactive force field for molecular dynamics simulations of hydrocarbon oxidation. The Journal of Physical Chemistry A 112 (5), 1040–1053.

Cumming, R.C., Andon, N.L., et al., 2004. Protein disulfide bond formation in the cytoplasm during oxidative stress. The Journal of Biological Chemistry 279 (21), 21749–21758.

Dietz, H., Rief, M., 2008. Elastic bond network model for protein unfolding mechanics. Physical Review Letters 100 (9), 098101.

Fernandes, P.A., Ramos, M.J., 2004. Theoretical insights into the mechanism for thiol/disulfide exchange. Chemistry-A European Journal 10 (1), 257–266.

Flory, P.J., 1953. Principles of Polymer Chemistry. Cornell University Press, Ithaca.

Fratzl, P., Weinkamer, R., 2007. Nature's hierarchical materials. Progress in Materials Science 52 (8), 1263–1334.

Garcia-Manyes, S., Liang, J., et al., 2009. Force-activated reactivity switch in a bimolecular chemical reaction. Nature Chemistry 1 (3), 236–242.

Grossfield, A., 2008. WHAM: the weighted histogram analysis method. http://membrane.urmc.rochester.edu/content/wham.

Hofbauer, F., Frank, I., 2010. Disulfide bond cleavage: a redox reaction without electron transfer. Chemistry-A European Journal 16 (17), 5097–5101.

Hogg, P.J., 2003. Disulfide bonds as switches for protein function. Trends in Biochemical Sciences 28 (4), 210–214.

Humphrey, W., Dalke, A., et al., 1996. VMD: visual molecular dynamics. Journal of Molecular Graphics 14 (1), 33.

Isralewitz, B., Gao, M., et al., 2001. Steered molecular dynamics and mechanical functions of proteins. Current Opinion in Structural Biology 11 (2), 224–230.

Keten, S., Buehler, M.J., 2008. Geometric confinement governs the rupture strength of H-bond assemblies at a critical length scale. Nano Letters 8 (2), 743–748.

Krishnan, R., Binkley, J.S., et al., 1980. Self-consistent molecular orbital methods. XX. A basis set for correlated wave functions. Journal of Chemical and Physics 72, 650.

Laioa, A., Parrinello, M., 2002. Escaping free-energy minima. Proceedings of the National Academy of Sciences of the United States of America 99, 12562–12566.

Leitner, V.M., Walker, G.F., et al., 2003. Thiolated polymers: evidence for the formation of disulphide bonds with mucus glycoproteins. European Journal of Pharmaceutics and Biopharmaceutics 56 (2), 207–214.

Li, W., Grater, F., 2010. Atomistic evidence of how force dynamically regulates thiol/disulfide exchange. Journal of the American Chemical Society 132 (47), 16790–16795.

Lv, L.-P., Xu, J.-P., et al., 2010. Disulfide-crosslinked biomimetic micelles: formation, thiol reactivity and cytotoxicity behavior. Macromolecular Chemistry and Physics 211 (21), 2292–2300.

MacKerell, A.D., Bashford, D., et al., 1998. All-atom empirical potential for molecular modeling and dynamics studies of proteins. The Journal of Physical Chemistry B 102 (18), 3586–3616.

Mayans, O., Wuerges, J., et al., 2001. Structural evidence for a possible role of reversible disulfide bridge formation in the elasticity of the muscle protein titin. Structure 9 (4), 331–340.

Mucke, N., Kreplak, L., et al., 2004. Assessing the flexibility of intermediate filaments by atomic force microscopy. Journal of Molecular Biology 335 (5), 1241–1250.

Napoli, A., Valentini, M., et al., 2004. Oxidation-responsive polymeric vesicles. Nature Materials 3 (3), 183–189.

Nielson, K.D., van Duin, A.C.T., et al., 2005. Development of the ReaxFF reactive force field for describing transition metal catalyzed reactions, with application to the initial stages of the catalytic formation of carbon nanotubes. The Journal of Physical Chemistry A 109 (3), 493–499.

Parbhu, A.N., Bryson, W.G., et al., 1999. Disulfide bonds in the outer layer of keratin fibers confer higher mechanical rigidity: correlative nano-indentation and elasticity measurement with an AFM. Biochemistry 38 (36), 11755–11761.

Perez-Jimenez, R., Li, J.Y., et al., 2009. Diversity of chemical mechanisms in thioredoxin catalysis revealed by single-molecule force spectroscopy. Nature Structural & Molecular Biology 16 (8), 890-U120.

Plimpton, S., 1995. Fast parallel algorithms for short-range molecular dynamics. Journal of Computational Physics 117 (1), 1–19.

Ponder, J.W., Case, D.A., et al., 2003. Force fields for protein simulations. In: Advances in Protein Chemistry, vol. 66. Academic Press, pp. 27–85.

Rahaman, O., van Duin, A.C.T., et al., 2011. Development of a ReaxFF reactive force field for glycine and application to solvent effect and tautomerization. The Journal of Physical Chemistry A 115 (2), 249–261.

Shewry, P.R., Tatham, A.S., 1997. Disulphide bonds in wheat gluten proteins. Journal of Cereal Science 25 (3), 207–227.

van Duin, A.C.T., Dasgupta, S., et al., 2001. ReaxFF: a reactive force field for hydrocarbons. The Journal of Physical Chemistry A 105 (41), 9396–9409.

Voet, D., Voet, J.G., 2004. Biochemistry. J. Wiley & Sons, New York.

Wang, H., Parry, D.A.D., et al., 2000. In vitro assembly and structure of trichocyte keratin intermediate filaments: a novel role for stabilization by disulfide bonding. The Journal of Cell Biology 151 (7), 1459–1468.

Wiita, A.P., Ainavarapu, S.R.K., et al., 2006. Force-dependent chemical kinetics of disulfide bond reduction observed with single-molecule techniques. Proceedings of the National Academy of Sciences of the United States of America 103 (19), 7222–7227.

Wiita, A.P., Perez-Jimenez, R., et al., 2007. Probing the chemistry of thioredoxin catalysis with force. Nature 450 (7166), 124–127.